ELSEVIER

Surface Science 436 (1999) 15–28

surface science

www.elsevier.nl/locate/susc

Reactions of N_2O_4 with ice at low temperatures on the Au(111) surface

Jiang Wang, Bruce E. Koel *

Department of Chemistry, University of Southern California, Los Angeles, CA 90089-0482, USA

Received 28 April 1998; accepted for publication 9 March 1999

Abstract

Reactions of N_2O_4, formed by condensation of NO_2 gas, with adsorbed water films as models for ice surfaces were studied on a Au(111) substrate at low temperatures under ultrahigh vacuum (UHV) conditions. Two thermal reaction paths were found, primarily by using infrared reflection–absorption spectroscopy (IRAS) and temperature programmed desorption (TPD) techniques. One path evolved gas phase HONO (nitrous acid) and HNO_3 (nitric acid) below 150 K, independent of both the crystallinity of the ice film and the exposure of NO_2. In contrast, another reaction pathway depended strongly on these variables and was conveniently monitored by the formation of oxygen adatoms on the Au(111) substrate surface. The latter reactions only occurred following multilayer adsorption of NO_2 (present as N_2O_4) and only if the adsorption was on amorphous ice clusters and not crystalline ice. The extent of these reactions was proportional to the concentration of 'free-OH' groups on the ice film, indicating that water molecules with only two hydrogen bonds were required to initiate these reactions by strongly hydrating N_2O_4. Following adsorption of N_2O_4 multilayers on amorphous ice, we propose that isomerization of $O_2N–NO_2$ (D_{2h}–N_2O_4) to $ONO–NO_2$ (nitrite–N_2O_4) occurs upon heating to 130–185 K. Further heating to 200–260 K leads to formation of $NO^+NO_3^-$ (nitrosonium nitrate). This compound is stable on the Au(111) surface up to at least 275 K. Decomposition of $NO^+NO_3^-$ on the Au(111) surface at 275–400 K evolves gas-phase NO_2, and possibly NO (nitric oxide), and also produces oxygen adatoms that recombine and thermally desorb as O_2 at about 520 K. These investigations provide new data on reactions of nitrogen oxides and condensed phases of water, which are of general importance for several technologies and improved understanding of atmospheric chemistry. In addition, new details are revealed concerning a novel method for producing oxygen adatoms on Au(111) surfaces under UHV conditions.

Keywords: Amorphous thin films; Catalysis; Chemisorption; Molecule–solid reactions; Nitrogen oxides; Physical adsorption; Surface chemical reaction; Thermal desorption spectroscopy; Vibrations of adsorbed molecules

1. Introduction

Interactions between water and nitrogen oxides in condensed phases play an important role in atmospheric chemistry and in a number of technologies. For example, N_2O_5 has been implicated in stratospheric ozone depletion because HNO_3 is produced at 185 K when N_2O_5 reacts with ice surfaces [1,2]. This reaction is a route for the formation of polar stratospheric clouds (PSCs) and serves to denitrify the stratosphere [1–4]. As another example, understanding reactions of NO_2-containing molecules in condensed phases is

* Corresponding author. Fax: +1-213-7403972.
E-mail address: koel@chem1.usc.edu (B.E. Koel)

0039-6028/99/$ – see front matter
PII: S0039-6028(99)00457-4

of general interest for the technology of energetic materials [5].

NO_2 (nitrogen dioxide) dissolves in water to exothermically form HNO_3 (nitric acid) and NO (nitric oxide). Nitric acid is a strong acid and powerful oxidizing agent, and concentrated nitric acid will oxidize most metals, except Au, Pt, Re, and Ir. There is quite a bit of mechanistic information about the reactions of NO_2 and water, and the hydrolysis of various oxides and oxyacids of nitrogen [6,7]. However, there is much less information about the interactions of these compounds with ice at low temperatures.

Only a few reports exist in the surface science literature about the low temperature coadsorption of H_2O and nitrogen oxides. Lazaga et al. and Bartram [8,9] made the first study of $NO_2 + H_2O$ reactions and found, surprisingly, that oxygen adatoms were formed on Au(111). Two recent reports have provided insight into the oxygen formation mechanism [10,11].

Experimental data establish that two thermal pathways exist for N_2O_4 reactions with ice at low temperatures. One path leads to acid formation and another eventually produces oxygen adatoms on Au(111). In this paper, based primarily on temperature programmed desorption (TPD) and infrared reflection–absorption spectroscopy (IRAS) data, we propose a reaction mechanism for this latter pathway in which ONO–NO_2 (nitrite–N_2O_4), formed via isomerization of strongly hydrated O_2N–NO_2 (D_{2h}–N_2O_4), converts to nitrosonium nitrate ($NO^+NO_3^-$) which decomposes to produce surface oxygen.

2. Experimental methods

These studies were carried out in a UHV chamber (2×10^{-10} Torr base pressure) equipped with a double-pass cylindrical mirror analyzer (CMA) for Auger electron spectroscopy (AES), reverse-view four-grid optics for low energy electron diffraction (LEED), a UTI 100 C quadrupole mass spectrometer (QMS) for TPD, and directed-beam gas dosers. A reaction antechamber was coupled directly to the top of the UHV chamber by a 2.75 in gate valve. The sample was positioned in the antechamber to carry out Ar^+ ion sputtering and perform FTIR studies in UHV or at higher pressures. IRAS was performed at a grazing angle of $\sim 86^\circ$ with a Mattson Galaxy 6020 FTIR spectrometer using two custom mirror-boxes. For these studies, a narrow-band, liquid-nitrogen cooled mercury cadmium telluride (MCT) detector was used. The IRAS spectra were collected with the Au(111) sample at 86 K using 8 cm^{-1} resolution and 1000 scans in a 4 min period. A clean surface spectrum was usually acquired after each adsorbate spectrum by annealing the Au(111) crystal to 550 K to desorb all adsorbates and quickly cooling to 86 K.

TPD measurements were made with the sample surface in line-of-sight to the QMS ionizer and using a linear heating rate of 3.5 K/s. Two highly transparent, fine Ni screens, one biased at -55 V and one at ground potential, were placed between the QMS ionizer and the sample to suppress low energy electrons coming from the QMS ionizer [12].

A polished Au(111) sample (10 mm diameter $\times$ 2 mm thickness) was mounted tightly under tension between two 0.015 in tungsten wires that were imbedded in two grooves along the crystal edges. These two wires were spot welded to thick Ta rods directly attached to a liquid N_2-cooled Cu block. The sample could be cooled to 85 K and resistively heated to 1000 K. The temperature was measured by a chromel–alumel thermocouple firmly pressed directly into a hole drilled in the edge of the sample. The Au(111) surface was cleaned by repeated sputtering–annealing cycles using Ar^+ ion sputtering at room temperature (10 min, 500 V, 1 μA) at an incident angle of 45° and annealing in vacuum at 973 K for 10 min. The cleanliness and order of the surface were checked by AES and LEED. Sharp spots characteristic of good ordering were always observed after annealing. Usually, a pattern due to the reconstructed Au(111) surface [13] was seen.

Deionized water (H_2O) was used after degassing via several freeze–pump–thaw cycles. NO_2 was used as received (Matheson, 99.9%). To minimize reactions of NO_2 in the doser gas lines, stainless steel and gold-plated gaskets were utilized, and the

entire dosing manifold gas line was initially passivated at $\sim 150^{\circ}C$ under NO_2 pressure for 30 min.

Adsorbate coverages herein are referenced to $\Theta = 1$ ML for the saturation monolayer coverage of a given adsorbate on the Au(111) surface. NO_2 monolayer coverages were determined by TPD, referenced to saturation of the chemisorbed NO_2 peak at 220 K [11,14] which was defined as $\Theta_{NO_2} = 1$ ML (or 4.2×10^{14} molecules/cm^2). The H_2O monolayer coverage is much less certain and was difficult to establish. Briefly, we used a background gas dose of H_2O sufficient to adsorb one-half of the molecules required for the water bilayer (1.0×10^{15} molecules/cm^2) found on Pt(111) [15] assuming unit sticking probability [10].

3. Results

3.1. Temperature programmed desorption (TPD)

Fig. 1 shows TPD spectra of H_2O taken after different exposures of NO_2 were given on a predeposited ice film formed by dosing 1 ML H_2O on Au(111) at 86 K. The bottom trace shows that H_2O desorption from Au(111), in the absence of NO_2 coadsorption, has only a single, narrow desorption peak at 163 K [16]. Water interacts very weakly with the Au(111) surface — TPD spectra of H_2O on Au(111) did not resolve the desorption of any strongly bound chemisorbed state. Also, no dissociation occurs during TPD. Physically, this ice monolayer is most likely comprised of relatively flat clusters extensively covering the surface. As shown later by using IRAS, this layer can be characterized as amorphous ice with 'free-OH' groups. It is important to point out here that the overall results presented in this paper did not change if the H_2O exposure used to form the ice film was increased by a factor of four. However, by keeping the amount of H_2O small, we could better observe the changes in the TPD spectra that were induced by NO_2 coadsorption.

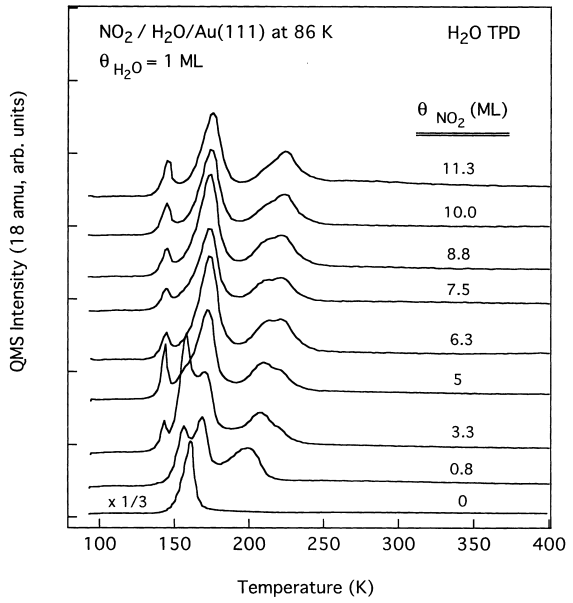

Fig. 1. H_2O TPD spectra following NO_2 exposures on an ice monolayer film on a Au(111) surface at 86 K. The bottom trace is for H_2O desorption from a 1 ML H_2O film on Au(111), in the absence of NO_2 coadsorption.

Exposing NO_2 on the ice film caused large changes in the H_2O desorption profile because of chemical reactions and hydration of nitrogen oxides and other reaction products. The H_2O TPD spectra were very similar following NO_2 exposures that produced $\Theta_{NO_2} = 6$ ML, and we interpret the interaction in these adlayers to be primarily between H_2O and N_2O_4, rather than with NO_2. There was no evidence in IRAS of any species other than H_2O and N_2O_4 in these layers at 86 K after dosing $\Theta_{NO_2} = 5$ ML (vide infra). We propose assignments for the new H_2O desorption peaks with $\Theta_{NO_2} = 6$ ML in Fig. 1. The peak at 144 K is lower in temperature than that for H_2O adsorbed on Au(111) in the absence of NO_2 coadsorption, as shown in the bottom trace, and so we propose that this peak arises from the desorption of acids such as HONO (nitrous acid) and HNO_3 (vide infra). H_2O desorption at 163 K is assigned to H_2O that is stabilized by hydrogen-bonding interactions with N_2O_4, and H_2O desorption at 215–225 K is attributed to H_2O produced from the decomposition of an intermediate formed by chemical reaction of N_2O_4 and 'free-OH' groups on the amorphous ice surface.

Tolbert et al. [1] observed H_2O desorption at 230 K when they studied N_2O_5 adsorption on ice surfaces and they attributed this to H_2O directly involved in the hydration of N_2O_5. Although the

structures and nitrogen oxidation states of N_2O_4 and N_2O_5 are different, we expect similar hydrogen bonding interactions of these two compounds with ice. Analogous hydrated species, such as $(N_2O_4)(H_2O)_x$ and $(N_2O_5)(H_2O)_y$, could be formed in each case at low temperatures. If so, TPD indicates that the hydration of N_2O_5 is stronger than that for N_2O_4 because of the higher H_2O desorption temperature for $(N_2O_5)(H_2O)_y$.

For $\Theta_{NO_2} < 3$ ML, the H_2O TPD spectra in Fig. 1 change strongly with NO_2 exposure. This may be because a mixture of N_2O_3 and N_2O_4 is formed at low NO_2 exposures, as based on IRAS (vide infra), and so additional interactions between NO_2 and N_2O_3 and ice could occur.

Fig. 2 shows the NO_2 TPD spectra obtained concomitantly with those in Fig. 1. As a reference, the bottom spectrum shows a NO_2 TPD spectrum following NO_2 adsorption directly on a clean Au(111) surface without any ice film. Other studies of NO_2 on Au(111) determined that NO_2 adsorption on Au(111) was completely reversible and that no decomposition occurred. NO_2 (bonded in an O,O′-chelating geometry) in the chemisorbed monolayer desorbed at 220 K and NO_2 from the physisorbed N_2O_4 multilayer desorbed at 144 K [11,14]. However, Fig. 2 shows that some irreversible reaction occurs during TPD that consumes NO_2 and/or N_2O_4 following NO_2 exposures on ice. A smaller amount of NO_2 desorption was observed from ice films than was observed from clean Au(111) for equivalent NO_2 exposures. This is most easily seen in Fig. 2 for the curves with $\Theta_{NO_2} < 5$ ML. Both the desorption peak at 143 K from N_2O_4 and the NO_2 desorption peak at 216 K from chemisorbed NO_2 were reduced for NO_2 adsorption on ice compared to clean Au(111). There was also a small peak at 169 K for $\Theta_{NO_2} = 5$ ML on ice that did not appear in the absence of H_2O coadsorption.

Intriguingly, the formation of oxygen adatoms on Au(111) under some conditions following coadsorption of NO_2 and H_2O has been reported [10,11]. Fig. 3 shows O_2 TPD spectra obtained simultaneously with the curves in Figs. 1 and 2. In the traces for $\Theta_{NO_2} = 5$ ML, O_2 desorbs at 505–520 K via recombination of oxygen adatoms [17].

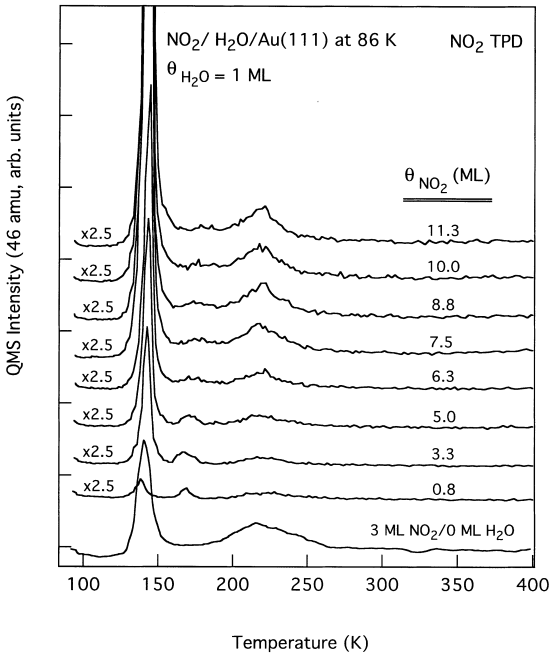

Fig. 2. NO_2 TPD spectra following NO_2 exposures on an ice monolayer film on a Au(111) surface at 86 K. The bottom TPD spectrum is for NO_2 desorption from a 3 ML NO_2 exposure on the Au(111) surface, in the absence of H_2O coadsorption.

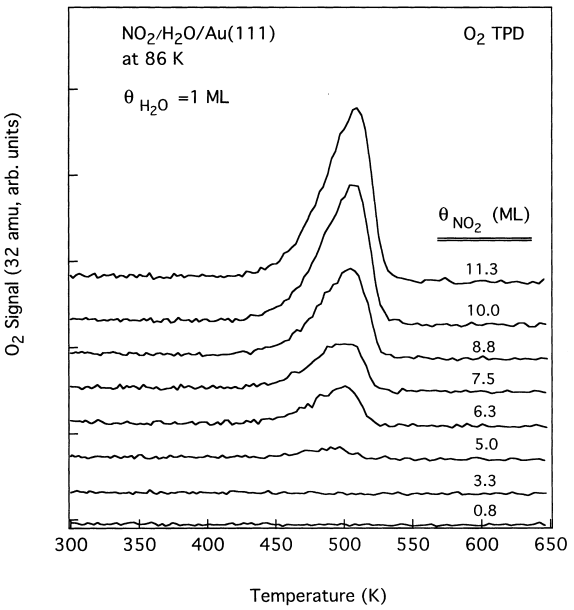

Fig. 3. O_2 TPD spectra following NO_2 exposures on an ice monolayer film on a Au(111) surface at 86 K.

The amount of O_2 desorbed increased with increasing NO_2 exposure, saturating at $\Theta_O = 0.42$ ML [with respect to the Au(111) surface atom density of 1.505×10^{15} atoms/cm^2] for the trace corresponding to $\Theta_{NO_2} = 10$ ML. Oxygen formation correlates with the high temperature H_2O desorption feature at 222 K in Fig. 1. Fig. 3 also shows that the nascent reaction intermediate(s) ultimately responsible for adsorbed oxygen formation are not formed by interactions with Au surface atoms. Otherwise, low exposures of NO_2 should have been more efficient at producing surface oxygen. We believe that the Au(111) substrate simply acts as an integrating detector for certain metastable reaction products that do not thermally desorb.

We attempted to detect many of the possible desorbed products from $N_2O_4 + H_2O$ reactions. No evidence was observed for gas-phase products such as H_2, N_2, NH_3, NH_2NH_2 and N_2O. Fig. 4 shows TPD traces observed following a 7.5 ML NO_2 exposure on a 1 ML H_2O film on Au(111) at 86 K. We propose that both HONO and HNO_3 are desorbed products. HONO is responsible for the 47 amu signal because we observe no signals attributable to larger molecules and HNO_3 does not give HONO nor HNO as cracking fragments [18]. HONO formation in the ionizer of the QMS cannot explain the desorption peak intensities at 47 amu which do not follow the NO or NO_2 desorption spectra, especially for a variety of dosing conditions. In addition to HONO, HNO_3 is also a desorbed product because HNO_3 gives a very small 63 amu signal. Reference spectra of gas-phase HNO_3 show a parent peak at 63 amu that is only $\sim 1\%$ of the largest peak (30 amu) in the QMS cracking pattern. The peak for the 63 amu signal is not at 143 K, as for the N_2O_4 multilayer, but at 148 K in Fig. 4. This is the same desorption temperature as observed previously for HNO_3 multilayers on Ag(110) [18]. Finally, HNO may also be a desorbed product and contribute to the 31 amu signal, but this is difficult to verify because the HONO fragmentation pattern is not available. Comparison of the 31 and 47 amu traces shows that the signal at 31 amu is not simply a cracking fraction of HONO.

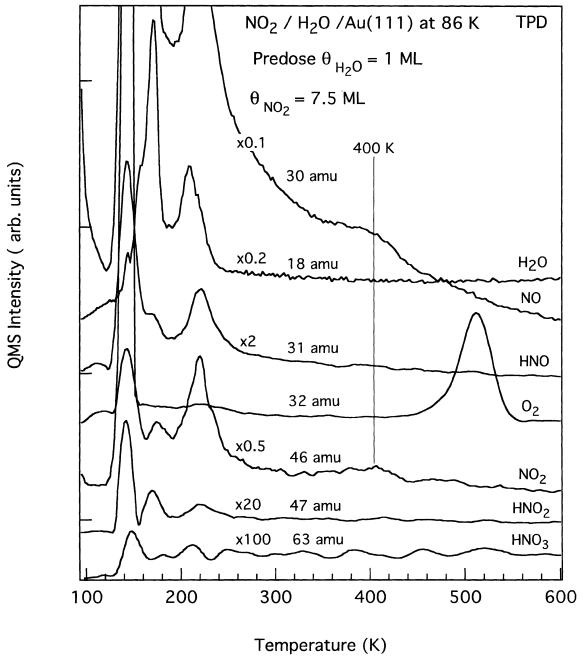

Fig. 4. TPD spectra for identifying desorbed products following NO_2 exposures on an ice monolayer film on Au(111) at 86 K.

Quantitative analysis shows that the amount of desorbed water after NO_2 exposures on the ice films of Fig. 1 is constant to within $\pm 25\%$. This leads us to conclude that the amount of hydrogen-containing products, e.g. HONO, HNO_3, or HNO, desorbed during these experiments is small.

In Fig. 4, the NO TPD peaks at 143, 174 and 222 K can be assigned to cracking from N_2O_4, HONO, or other species. The high temperature NO desorption feature near 400 K is unusual, and is not caused by desorption of chemisorbed NO [14].

For the NO_2 TPD spectrum shown in Fig. 4, we assign the origin of the peak at 143 K to decomposition of unreacted N_2O_4 in the multilayer, that at 174 K to a cracking fraction of HONO, and the peak at 222 K to chemisorbed NO_2 that is formed on Au(111) during heating in TPD. The NO_2 TPD spectra also have an unusual high temperature feature near 400 K. There is no H_2O desorption over this temperature range, and so this is clear evidence of NO_2 (and possibly a small amount of NO) evolution from the decomposition of intermediates that contain no hydrogen but finally produce oxygen adatoms on Au(111).

Several additional TPD measurements were made to elucidate conditions for producing the reactive intermediate that decomposed to form surface oxygen. The O_2 TPD yield was a convenient monitor for these conditions. In one set of experiments (not shown), O_2 TPD spectra were obtained after dosing 7.5 ML NO_2 on ice films of different initial thickness (0.3, 0.5, 2, 3, and 4 ML H_2O) predeposited on the Au(111) surface at 86 K. The amount of O_2 desorbed during TPD in these experiments was constant, independent of the initial thickness of the ice film used for NO_2 adsorption. These results indicate that the reactive intermediate that ultimately decomposes to form oxygen adatoms on Au(111) is formed only at the outer surfaces of ice clusters and is not specifically formed by the Au(111) surface. In other separate experiments, we found that the amount of oxygen formed from N_2O_4+ice reactions was not affected by the dosing sequence (i.e. N_2O_4 first or H_2O first) nor the defect concentration at the Au(111) surface [10].

Surface oxygen formation is highly dependent on the substrate temperature during coadsorption [10]. Fig. 5 clearly illustrates this influence. O_2 desorption spectra are shown following identical doses of 7.5 ML NO_2 on an ice film produced by exposure of 1 ML H_2O on Au(111) at 86 K in each case. The only difference in this series was that the ice film was preannealed for 0.5 min to different temperatures prior to the NO_2 exposures. The amount of oxygen produced by reactions during TPD decreased as the preannealing temperature of the ice increased. Reactions of N_2O_4 with ice grown at 86 K without any annealing produced the maximum amount of oxygen. No oxygen desorption was detected if the ice film had been preannealed above 110 K. In the next section, we utilize vibrational spectroscopy to probe the changes in the ice film that occur over this temperature range and play such an important role in forming the intermediate that leads to oxygen formation.

As a final point, we rule out oxygen formation simply arising from deposition of some impurity that accompanies NO_2 dosing. Among other reasons, Fig. 5 shows that O_2 desorption can be eliminated by preannealing the ice film but keeping

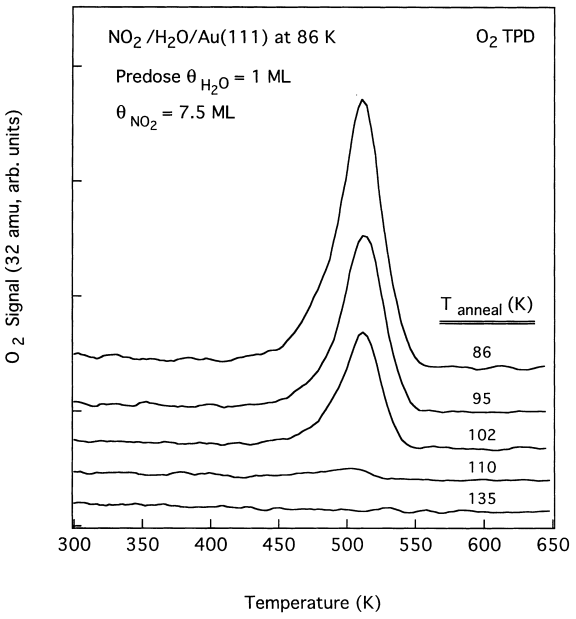

Fig. 5. O_2 TPD spectra following 7.5 ML NO_2 exposures on ice monolayer films on Au(111) at 86 K. The important variable probed is the preannealing temperature of the ice films prior to NO_2 exposures. Following the deposition of 1 ML H_2O on a Au(111) surface at 86 K, the substrate was annealed to the indicated temperature for 30 s, and then exposed to NO_2 with the substrate at 86 K.

the NO_2 (along with any impurity) exposure constant with the substrate at 86 K.

3.2. Infrared reflection absorption spectroscopy (IRAS)

The condensed water film grown below 100 K can be characterized as amorphous ice because of a broad peak at 3400 cm^{-1} and a small sharp peak at 3740 cm^{-1} in the IRAS spectra in Fig. 6 [19,20]. The OH stretching mode of water molecules that are fully (four-coordinated) involved in hydrogen bonding gives rise to the strong broad peak, while the small sharp peak is due to OH stretching modes in water molecules that have an OH group not involved in hydrogen bonding. H_2O molecules giving rise to this 'free-OH' vibration at 3740 cm^{-1} have been characterized by Buch and Devlin [21] using spectroscopic and computational methods. They concluded that the 'free-OH' band at 3730 cm^{-1} comes from two-coordinated water

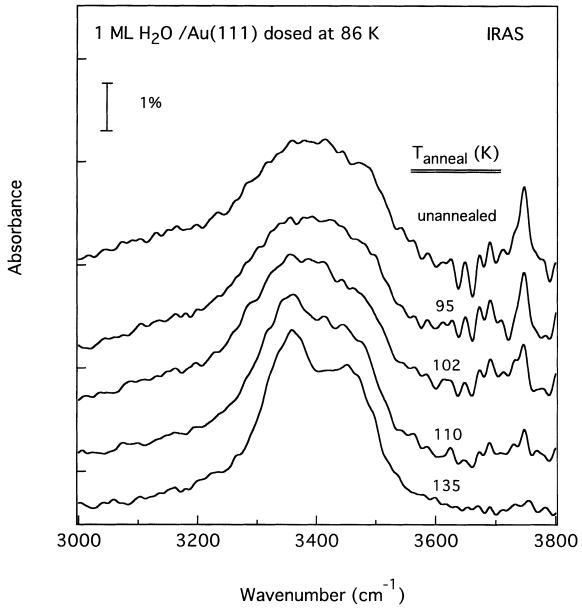

Fig. 6. IRAS spectra obtained after dosing 1 ML H_2O on a Au(111) surface at 86 K and then annealing the ice monolayer film to the indicated temperature for 30 s. All of the spectra were collected with the substrate at 86 K.

molecules in amorphous ice, i.e. H_2O molecules that use the oxygen and one hydrogen atom to form two hydrogen bonds with neighboring water molecules. They also concluded that 'free-OH' species are mostly distributed on the surface of amorphous ice. In Fig. 6, the 'free-OH' peak decreased as the annealing temperature was increased, disappearing between 110 and 135 K. We attribute the disappearance of the 'free-OH' peak and the evolution of two peaks at 3350 and 3450 cm^{-1} to the sintering of small ice particles or partial crystallization of amorphous ice [19–21]. This is also consistent with a previous assignment of crystalline ice and the phase transition temperature [22]. By comparison with Fig. 5, one can show that the amount of oxygen formed from the coadsorbed film during TPD is correlated to the amount of 'free-OH' species, presumably on the ice surface.

In order to probe the chemical nature of the adsorbed layer produced by NO_2 exposures on ice films, and to identify reaction intermediates that lead to the products seen in TPD, two different IR 'warm-up' studies were performed. The first utilized post-dosing 1 ML NO_2 on a 1 ML H_2O film on Au(111) at 86 K, where the ice film was grown with the substrate at 86 K. This procedure did not generate O_2 desorption in TPD. IRAS spectra starting with such a coadsorbed layer are shown in Fig. 7. A monolayer exposure of NO_2 produced a mixed layer of N_2O_3 and N_2O_4 on the ice film at 86 K. N_2O_3 (O_2N–NO) was identified by three bands at 1185, 1276, and 1900 cm^{-1} due to the $\nu_s(NO_2)$, $\nu_{as}(NO_2)$, and $\nu(N{=}O)$ modes, respectively [11,14,23–25]. D_{2h}–N_2O_4 (O_2N–NO_2) was identified by three bands at 1276, 1520 and 1746 cm^{-1} originating from the $\nu_s(NO_2)$, $2\delta(NO_2)$ combination, and $\nu_{as}(NO_2)$ modes, respectively [11,14,23–25]. Heating to 220 K eliminates all but one weak band at 1175 cm^{-1} that we assign to the $\nu_s(NO_2)$ mode of chelating NO_2 chemisorbed on the Au(111) surface [14]. No vibrational bands from any adsorbates were detected after heating the substrate to 275 K.

The film formed from a 10 ML NO_2 exposure

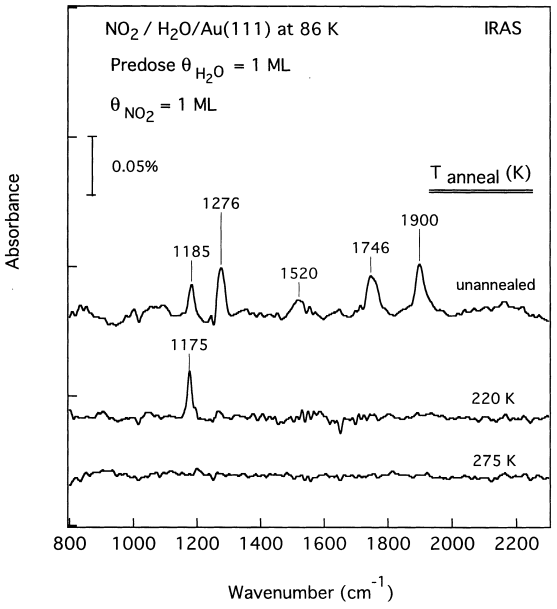

Fig. 7. IRAS 'warm-up' spectra obtained after sequentially heating the substrate to the indicated annealing temperatures. A 1 ML NO_2 exposure was given on an ice monolayer film on Au(111) at 86 K, and then the substrate was annealed to the indicated temperature for 30 s. All of the spectra were collected with the substrate at 86 K.

on a predosed ice monolayer on Au(111) at 86 K was investigated also by IRAS as the substrate was warmed gradually to 400 K. This dosing procedure caused a substantial amount of O_2 desorption in TPD as was shown in Fig. 3. These IRAS 'warm-up' spectra are provided in Fig. 8. The spectra are remarkably different from those shown in Fig. 7. A N_2O_4 film exists on the ice surface from 86 to 130 K. Four bands at 783, 1298, 1735 and 1760 cm^{-1} in the spectrum at 86 K are assigned to the $\delta_s(NO_2)$, $\nu_s(NO_2)$ and $\nu_{as}(NO_2)$ modes, respectively, of solid N_2O_4. We have no explanation for the splitting of the $\nu_{as}(NO_2)$ band, but similar results were seen previously in IR studies of solid N_2O_4 [11,23]. When this N_2O_4 film on ice was heated to 130 K, the vibrational bands red-shifted to 775, 1284, 1728, 1749 cm^{-1}, respectively. We interpret this shift as indicative of a stronger interaction between N_2O_4 and ice at 130 K compared to 86 K. The sharpness of the bands is indicative of highly crystalline ordering of the solid N_2O_4 adlayer [26]. Also, the $\nu_s(NO_2)/\nu_{as}(NO_2)$ intensity ratio for the N_2O_4 film on ice at 86–130 K was about 8, and this can be compared to the same IR intensity ratio for gas-phase N_2O_4 which is about 1 [27]. Such a change in relative band intensities is often indicative of a preferred orientation in the adlayer, because the IR metal–surface selection rule [28] states that the absorption due to dynamic dipoles parallel to the metal surface is strongly diminished while that for dynamic dipoles perpendicular to the surface is enhanced. The $\nu_s(NO_2)$ mode in D_{2h}–N_2O_4 has a dynamic dipole oriented parallel to the N–N bond, whereas the $\nu_{as}(NO_2)$ mode has its dynamic dipole oriented perpendicular to the N–N bond [29]. Thus, Fig. 8 shows that the five-layer thick crystalline N_2O_4 film on ice at 86–130 K has a preferred orientation with the N–N bond in D_{2h}–N_2O_4 almost perpendicular to the surface of the Au(111) substrate. The orientation of N_2O_4 directly in contact with water molecules in the ice layer could be quite different because the absorption from these species could be overwhelmed by the N_2O_4 multilayer bands and no vibrations with dynamic dipoles parallel to the Au(111) surface can be observed due to screening effects. One explanation for the observed splitting of the $\nu_{as}(NO_2)$ band mentioned above could be N_2O_4 species in direct contact with the ice layer.

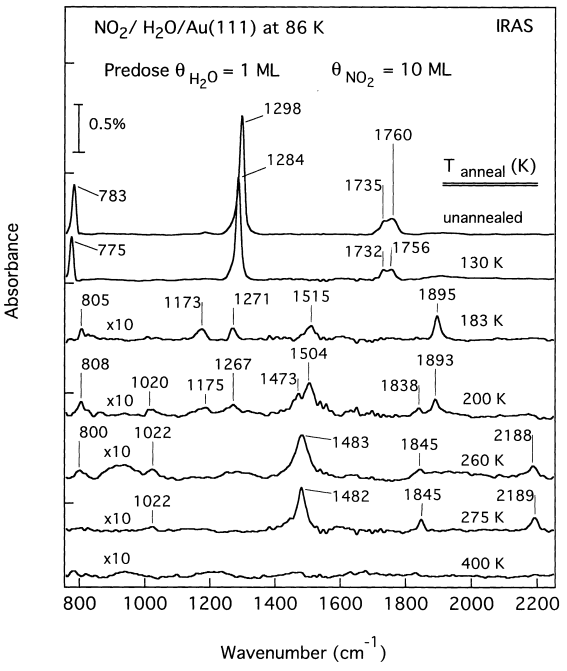

Fig. 8. IRAS 'warm-up' spectra obtained after sequentially heating the substrate to the indicated annealing temperatures. A 10 ML NO_2 exposure was given on an ice monolayer film on Au(111) at 86 K, and then the substrate was annealed to the indicated temperature for 30 s. All of the spectra were collected with the substrate at 86 K.

As shown in Fig. 8, increasing the temperature to 183 K caused several new absorption bands to appear at 805, 1173, 1271, 1515 and 1895 cm^{-1}. The strongest one at 1515 cm^{-1} cannot be assigned to NO, N_2O_3, N_2O_4 or N_2O_5 because these species have no fundamental vibrational modes at this energy and combination bands are usually very weak [30]. This band is often attributed to some species with an NO_3 group [30]. On this basis, we assign all of the bands (at 805, 1173, 1271, 1515 and 1895 cm^{-1}) to two conformers, D and D′ [31–33], of nitrite–N_2O_4 (ONO–NO_2), as given in Table 1.

Warming this adlayer to 200 K caused new bands at 1020, 1473, and 1838 cm^{-1} to appear. The 1020 cm^{-1} band is assigned to a main band for the NO_3^- anion [34]. This means that a new

Table 1
Assignments of vibrational frequencies (cm^{-1}) of nitrite–N_2O_4 ($ONONO_2$)

Mode		$ONONO_2$		$ONONO_2$/Au(111)	
Assignment	Symmetry (for C_s)	Oxygen matrix IR [31,32]		IRAS (this work)	
		D	D′	183 K	200 K
ν(N=O)	A′	1829	1889	1895	1838, 1893
$\nu_a(NO_2)$	A′	1645	1584	1515	1504, 1473
$\nu_s(NO_2)$	A′	1291	1290	1271	1267
ν(N–O)	A′	905	916		1020
$\delta(NO_2)$	A′	783	794	805	808

intermediate coexists with nitrite–N_2O_4 after heating to 200 K.

Fig. 8 shows that annealing this adlayer to 260 or 275 K results in a spectrum with five bands, at 800, 1022, 1482, 1845, and 2189 cm^{-1}. These are assigned to adsorbed $NO^+NO_3^-$ (nitrosonium nitrate) [31–33] as shown in Table 2. Bands at 1022 and 1482 cm^{-1} are due to the $\nu_s(NO_3^-)$ and $\nu_{as}(NO_3^-)$ modes, respectively. The band at 1845 cm^{-1} is due to a $\nu_s(NO_3^-)+\delta(NO_3^-)$ combination band of $NO^+NO_3^-$ ($1032+800\ cm^{-1}$). The 2189 cm^{-1} band is in the 2150–2300 cm^{-1} range that is characteristic of NO^+ (nitrosonium ion) [35]. The assignment of this band to an NO^+ stretching mode confirms the identification of the $NO^+NO_3^-$ intermediate. Table 2 gives the vibrational frequencies in the Raman spectrum of $Cu(NO_3)_3^-NO^+$ [33]. With this support, along with the fact that NO molecules do not adsorb on Au(111) at 86 K [14], this is a pretty clear identification. Some differences between the vibrational frequencies for the $NO^+NO_3^-$ species in Table 2 are expected. The $\nu_{as}(NO_3)$ frequency is highly dependent on the geometry and charge of NO_3 [36]. Free NO_3^- has $\nu_{as}(NO_3^-)=1390\ cm^{-1}$, but this usually shifts to higher frequency when its negative charge is balanced by cations. The $\nu_{as}(NO_3^-)$ mode is at 1460 cm^{-1} in alkali metal nitrates, but this frequency is highly dependent on the type of cation [37].

4. Discussion

The thermal chemistry following NO_2 exposures and condensation of N_2O_4 on ice films at temperatures of 86 K and above is quite complex. As one indication, desorption of H_2O from these films as the temperature is raised occurs in as many as five peaks in TPD. In addition, a large number of

Table 2
Assignments of vibrational frequencies (cm^{-1}) of nitrosonium nitrate ($NO^+NO_3^-$)

Mode		$NO^+NO_3^-$			$Cu(NO_3)_3^-NO^+$	$NO^+NO_3^-$/Au(111)	
Assignment	Symmetry (D_{3h} for NO_3^-)	Amorphous IR [33]	Crystalline IR [33]		Raman [33]	IRAS (this work)	
						260 K	275 K
$\nu(NO^+)$	A′	2149	2263	2245	2236	2188	2189
$\nu_s(NO_3^-)+\delta(NO_3^-)$			1760	1752			
$\nu_a(NO_3^-)$	E′	1438		1429	1511	1483	1482
$\nu_a(NO_3^-)$	E′	1385	1355	1372	1282		
$\nu_s(NO_3^-)$	A_1'	1028	1041	1041	1059	1022	1022
$\delta(NO_3^-)$	A_2''	816	826	815		800	
$\delta(NO_3^-)$	E′		716	713			

vibrational bands were observed in IRAS at 130–180 K which indicates a complex composition for these layers. Nonetheless, several observations can be made. Nitrous acid (HONO), and possibly nitric acid (HNO_3), desorption was observed at temperatures below 150 K during TPD measurements. Acid formation does not depend strongly on the conditions used to form the NO_2+H_2O coadsorbed layer. Under conditions that produce N_2O_4 condensation on amorphous ice films that have 'free-OH' groups, heating caused the formation of $ONO–NO_2$ and $NO^+NO_3^-$. These species were identified by IRAS. We postulate that strong hydration facilitates isomerization of N_2O_4 ($O_2N–NO_2 \leftrightarrow ONO–NO_2$). Nitrite–$N_2O_4$ converts thermally to $NO^+NO_3^-$. We propose that this species then decomposes via direct interaction with the Au(111) substrate to desorb NO_2, and possibly NO, and to produce oxygen adatoms. These oxygen formation reactions occur by a separate pathway from the acid formation reactions.

4.1. Reaction mechanisms

Acid formation in these experiments represents expected chemistry. NO_2, N_2O_3 and N_2O_4 interact with water at room temperature at atmospheric pressure to form HNO_2 and HNO_3 [38,39]. When NO_2, N_2O_3 and N_2O_4 react with ice, we find that HONO and HNO_3 are desorbed as gas-phase products during subsequent heating. These acid formation reactions occur below 150 K with little activation energy barrier, and do not depend either on the crystallinity of the ice or the NO_2 exposures. We assume that these reactions and those with water at room temperature occur via similar mechanisms.

In sharp contrast to the acid formation reactions, reactions that lead ultimately to oxygen formation are highly sensitive to the crystallinity of the ice and the NO_2 exposure. Only multilayers of N_2O_4 react with amorphous ice to eventually generate oxygen adatoms on the Au(111) surface. We believe that this establishes that surface oxygen is not formed by the same reactions that produce nitrous and nitric acid. Based on our IRAS measurements, we propose the following reaction mechanism for oxygen formation:

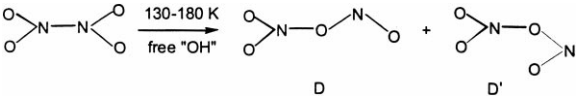

$$\mathrm{D\ and\ D'} \xrightarrow{200\text{–}260\ \mathrm{K}} \mathrm{NO^+NO_3^-}$$

$$\mathrm{NO^+NO_3^-} \xrightarrow{275\text{–}400\ \mathrm{K}} \mathrm{NO(g)+NO_2(g)+O_a}$$

$$\mathrm{2O_a} \xrightarrow{520\ \mathrm{K}} \mathrm{O_2(g)}.$$

NO_2 desorption, and possibly a small amount of NO desorption, in the 350–450 K temperature range in the TPD data of Fig. 4 supports this mechanism. NO is a large peak in the NO_2 cracking pattern, and so it is not clear if NO is a product because we have not quantified all of the product yields. NO_2 and NO desorption at 350–450 K is limited by the rate of $NO^+NO_3^-$ decomposition because NO_2 desorbs at 230 K following NO_2 exposures on Au(111), and NO desorbs below 86 K on Au(111) because no NO uptake was observed after NO exposures [14,23]. The absence of any H_2O desorption in this temperature range is also consistent with the decomposition of intermediates that do not contain hydrogen.

In a set of related studies, we investigated reactions of H_2O with predosed NO_2 films on Au(111) [11]. Only large NO_2 exposures that produced multilayers, i.e. films of N_2O_4, reacted with subsequently dosed water to produce surface oxygen (if the water was dosed with the substrate below 110 K). Warming the films produced by water exposures on either submonolayer and monolayer amounts of chelating NO_2 preadsorbed on Au(111) or a pure N_2O_3 monolayer preadsorbed on Au(111) did not generate surface oxygen, even if the substrate temperature was below 110 K to condense water into amorphous ice. These results are consistent with the mechanism proposed above, and further demonstrate that N_2O_4 is the only reactant responsible for oxygen formation. These experiments also support our conclusion that the Au(111) surface only functions as an inert support and an integrating

detector for intermediates, rather than playing a direct role in the generation of reactive species at low temperatures.

We do not believe that HONO and HNO_3 are precursors for oxygen adatom formation on Au(111) in these experiments. First, formation of HONO and HNO_3 is independent of NO_2 exposure and crystallinity of the ice, while the oxygen formation reaction is very sensitive to these variables. Second, no evidence for HONO or HNO_3 was observed in IRAS spectra at temperatures above 180 K under conditions that lead to oxygen formation. We compared our spectra to the IR spectra of gas-phase HONO and gaseous and adsorbed HNO_3 [40–42]. Furthermore, when a mixture of $H_2O + NO_2$ (premixed in the gas lines at 300 K) was used to condense films onto Au(111) at 86 K, no O_2 desorption was observed in subsequent TPD spectra. HONO and HNO_3 are formed when gaseous H_2O and NO_2 are mixed at room temperature, and so our conclusion is that these species are not involved in oxygen formation on Au(111). However, oxygen adatoms are produced by dissociative adsorption of nitric acid on the Ag(110) surface [18].

It has been proposed that a small amount of HOONO (peroxynitrous acid) was formed, in addition to HNO_3, when gaseous H_2O and NO_2 was mixed at 300 K [43]. IR spectra of matrix-isolated samples of HOONO in solid Ar have peaks at 3546, 1704, 1364, 952 and 773 cm^{-1} [44]. There was no evidence in any of our IRAS spectra for the formation of HOONO.

We searched for the desorption of various possible reduction products during TPD, but did not find any. No H_2, N_2, NH_3, NH_2NH_2, or N_2O was desorbed. Thus, we rule out formation of oxygen adatoms via oxidation of H_2O by nitrogen oxides.

Transitory formation of $NO^+NO_3^-$ was observed previously to occur in reactions involving N_2O_4 in solvents of high dielectric constant [45,46]. $NO^+NO_3^-$ was postulated to arise from the following reaction [45,47]:

$$O_2N\text{–}NO_2 \rightarrow ONO\text{–}NO_2 \rightarrow NO^+NO_3^-.$$

Also, Pinnick et al. [48] and Agnew et al. [49] observed N_2O_4 isomerization using FTIR in a diamond-anvil cell under high pressures, and found that moderate heating (< 373 K) and pressures above 1.0 GPa resulted in conversion of N_2O_4 to $NO^+NO_3^-$. Our proposed mechanism is consistent with these observations. We believe that the role of highly polar, 'free-OH' groups on amorphous ice is to facilitate isomerization of $O_2N\text{–}NO_2$ to $ONO\text{–}NO_2$.

One might consider whether H_2O is required at all to form $NO^+NO_3^-$ because a number of studies by Loewenschuss and coworkers [33,50–53] show that a tiny amount of nitrite–N_2O_4 and $NO^+NO_3^-$ can be produced from condensing NO_2 at very low temperatures (~20 K) on an inert matrix. Heating this condensed film to higher temperature (150 K) yields more $NO^+NO_3^-$. However, these reactions apparently only occur at very low dosing temperatures. Only crystalline D_{2h}–N_2O_4 was found, and no nitrite–N_2O_4 or $NO^+NO_3^-$ was detected, when NO_2 was condensed on copper and gold-coated copper surfaces above 80 K. Koch et al. [54] also did not observe nitrite–N_2O_4 or $NO^+NO_3^-$ in IRAS studies of NO_2 dosed on Au foil at 80 or 120 K. However, when NO_2 was dosed at a slow rate onto copper or gold-coated copper surfaces at 20 K, amorphous N_2O_4 and $ONO\text{–}NO_2$ was formed and $NO^+NO_3^-$ was clearly observed by Raman and FTIR upon annealing to 205 K [51]. Thus, $NO^+NO_3^-$ was formed from $ONO\text{–}NO_2$, which was previously formed from amorphous D_{2h}–N_2O_4.

IRAS clearly reveals that thick films of adsorbed N_2O_4, on either a predosed ice film or on clean Au(111), have a preferred alignment with the N–N bond nearly perpendicular to the Au substrate surface. But, this orientation may not reflect the N_2O_4 molecules perturbed by hydrogen bonding to ice at the interface. The discussion above illustrated the important role of amorphous N_2O_4. And so, the layer of reacting N_2O_4 at the ice interface could be amorphous. N_2O_4 molecules should strongly participate in hydrogen bonding with 'free-OH' groups of amorphous ice and may even incorporate into the ice film.

Because the formation of $ONO\text{–}NO_2$ and $NO^+NO_3^-$ is enhanced by disordered ice structures, procedures that grow highly disordered ice or small amorphous ice nanoclusters could pro-

duce more surface oxygen than we obtained ($\Theta_O = 0.42$ ML) [10]. A similar comment could be made about amorphous N_2O_4. Lower dosing temperatures or larger dosing rates may be simple ways to generate more of these species on Au(111) from the coadsorption of $H_2O + NO_2$. This could be of practical importance for preparing higher oxygen coverages on Au(111) by this method.

4.2. Hydrogen bonding effects on isomerization of O_2N–$NO_2 \leftrightarrow ONO$–NO_2

The thermodynamics of isomerization of O_2N–$NO_2 \leftrightarrow ONO$–NO_2 were reported by Pinnick et al. [48] for a number of pressures and temperatures. They found $\Delta H = 18.8 \pm 3.9$ kJ/mol, $\Delta G = 18.8 \pm 4.1$ kJ/mol, and $\Delta S = 0 \pm 4.2$ J/mol K under conditions of $P \sim 0$ GPa and $T = 298$–350 K. Isomerization is not sensitive to pressure at 289–450 K, but the conversion of ONO–NO_2 to $NO^+NO_3^-$ is more favorable under higher pressures. This is because the latter reaction entails charge-separation and has a negative activation volume. We do not know of any thermodynamic data on the conversion of ONO–NO_2 to $NO^+NO_3^-$, or on the isomerization of O_2N–NO_2 to ONO–NO_2, at lower temperatures. Certainly no thermodynamic data is available for these reactions at interfaces.

Several studies have shown previously that Au(111) [11,14] or Au(poly) [54] surfaces do not substantially promote the isomerization of O_2N–NO_2 to ONO–NO_2. No ONO–NO_2 was detected prior to the desorption of N_2O_4 near 140 K. The IRAS results presented herein show that the nitrite–N_2O_4 isomer exists prior to the formation of oxygen on Au(111), and so it is likely that it is an essential precursor for this reaction. 'Free-OH' groups on ice surfaces evidently facilitate this isomerization better than gold surfaces. We propose that strong hydrogen bonding between N_2O_4 and the highly polar 'free-OH' groups on amorphous ice surfaces plays a crucial role in breaking the N–N bond [$D(O_2N$–$NO_2) = 12.6$ kcal/mol] and stabilizing polar products and intermediates such as ONO–NO_2 and $ON^+NO_3^-$.

Because an 'upright' N_2O_4 molecule on an ice surface could involve two hydrogen bonds, and two more could occur if a 'flat-lying' or incorporated species were formed, a substantial interaction energy between N_2O_4 and H_2O molecules could exist. The strength of the hydrogen bond in ice and water is generally estimated to be 3.6–6.0 kcal/mol [55]. If we assume a similar hydrogen bonding interaction occurs between N_2O_4 and ice, then the total hydrogen bonding interaction is in the range of 7–24 kcal/mol. This estimate should be a lower limit, and so hydrogen-bonding interactions could account for stabilizing the cleavage of N–N bond in O_2N–NO_2 to form nitrite–N_2O_4. For example, the much stronger O–Cl bond in $ClONO_2$ [$D(Cl$–$ONO_2) = 48$ kcal/mol] can be cleaved by hydrolysis resulting from the formation of hydrogen bonds when $ClONO_2$ is incorporated into ice films [56]. Hydrogen bonding interactions strongly stabilize charged intermediates like $ON^+NO_3^-$. For example, the strong bond in HCl [$D(H$–$Cl) = 103$ kcal/mol] is readily ionized when HCl is incorporated into ice films [57].

5. Conclusions

Thermal reactions following the condensation of NO_2 on ice films were studied on a Au(111) substrate under UHV conditions. Small exposures of NO_2 on ice at 86 K led to the formation of D_{2h}–N_2O_4 (O_2N–NO_2) from dimerization of NO_2 and some N_2O_3 (via reaction with background NO gas). Larger exposures of NO_2 on ice at 86 K formed pure crystalline layers of D_{2h}–N_2O_4 with a preferential orientation of the N–N bond perpendicular to the surface of the Au(111) substrate. No evidence was observed for nascent reactions between any nitrogen oxides and H_2O at 86 K on these ice films. Two low-temperature reaction pathways were observed upon heating above this temperature. One reaction channel was detected by mass spectrometry using TPD and produces gas-phase HONO, and possibly HNO_3, below 150 K. These facile reactions proceed regardless of the crystallinity of the ice film and the NO_2 film thickness. Another reaction channel can be accessed only if relatively large NO_2 exposures occur on an amorphous ice film containing 'free-

OH' groups. IRAS was used to follow the concentration of these 'free-OH' groups, which arise from water molecules that are not fully involved in H-bonding within the ice film. IRAS was used also to identify the reaction intermediates and products from subsequent reactions following NO_2 exposures on the ice films. For amorphous ice films containing 'free-OH' groups, i.e. ice films that had grown never exceeding 110 K, strong hydration of N_2O_4 occurs which facilitates the isomerization of $O_2N–NO_2$ to $ONO–NO_2$ at temperatures of 130–180 K. $ONO–NO_2$ then forms the ion-pair compound $NO^+NO_3^-$ at 200–260 K. Upon heating to 275–400 K, adsorbed $NO^+NO_3^-$ decomposes to form oxygen adatoms on Au(111). O_2 evolution eventually occurs at 520 K via recombinative desorption to leave a clean Au(111) substrate.

These reactions reveal fundamental interactions of oxides of nitrogen and H_2O that are needed to improve the understanding of atmospheric chemistry and reactions related to energetic materials. In a more direct application, we have now mapped out the conditions and reaction mechanism for a novel and convenient method to oxidize gold under UHV conditions at low temperatures. This should facilitate future surface science studies of selective oxidation chemistry and catalysis on Au surfaces.

Acknowledgements

This work was supported by the Army Research Office.

References

[1] M.A. Tolbert, M.J. Rossi, D.M. Golden, Science 240 (1988) 1018.
[2] R.P. Wayne, I. Barnes, P. Biggs, J.P. Burrows, C.E. Canosa-Mas et al., Atmos. Environ. 25A (1) (1991) 1.
[3] B.J. Gertner, J.T. Hynes, Science 271 (1996) 1563.
[4] S. Solomon, R.R. Garcia, F.S. Rowland, D.J. Wuebbles, Nature 321 (1986) 755.
[5] T.B. Brill, K.J. James, Chem. Rev. 93 (1993) 2667.
[6] F.A. Cotton, G. Wilkinson, Advanced Inorganic Chemistry, Wiley Interscience, New York, 1988.
[7] G.K.S. Prakash, L. Heiliger, G.A. Olah, Inorg. Chem. 19 (1990) 4965.
[8] M.A. Lazaga, D.H. Parker, G.N. Kastanas, B.E. Koel, S.T. Oyama, J.W. Hightower (Eds.), ACS Symp. Series 523 (1993) 90.
[9] M.E. Bartram, Ph.D. Thesis, University of Colorado, Boulder, CO, 1982.
[10] J. Wang, M.R. Voss, H. Busse, B.E. Koel, J. Phys. Chem. B102 (1998) 4693.
[11] J. Wang, B.E. Koel, J. Phys. Chem. A102 (1998) 8573.
[12] C. Xu, B.E. Koel, Surf. Sci. 292 (1993) L803.
[13] D.L. Abernathy, D. Gibbs, G. Grubel, K.G. Huang, S.G.J. Mochrie, A.R. Sandy, D.M. Zehner, Surf. Sci. 283 (1993) 260.
[14] M.E. Bartram, B.E. Koel, Surf. Sci. 213 (1989) 137.
[15] F.T. Wagner, T.E. Moylan, Surf. Sci. 182 (1987) 125.
[16] B.D. Kay, K.R. Lykke, J.R. Creighton, S.J. Ward, J. Chem. Phys. 91 (1989) 5120.
[17] N. Saliba, D.H. Parker, B.E. Koel, Surf. Sci. (1999) in press.
[18] R. Dohl-oelze, C.C. Brown, E.M. Stuve, Surf. Sci. 210 (1989) 339.
[19] B. Rowland, M. Fisher, J.P. Devlin, J. Phys. Chem. 97 (1993) 2485.
[20] M.J. Wojcik, V. Buch, J. Chem. Phys. 99 (1993) 2332.
[21] V. Buch, J.P. Devlin, J. Chem. Phys. 94 (1991) 4091.
[22] J.E. Schaff, J.T. Roberts, J. Phys. Chem. 98 (1994) 6900.
[23] D.M.L. Goodgame, K. Baberschke, Phys. Rev. B 36 (1965) 5756.
[24] I.C. Hisatsune, J.P. Devilin, Spectrochim. Acta 16 (1960) 401.
[25] E.T. Arakawa, C.H. Wilkins, Anal. Chem. 24 (1952) 1253.
[26] G.R. Smith, W.A. Guillory, J. Mol. Spectrosc. 68 (1977) 223.
[27] C.H. Bibart, G.E. Ewing, J. Chem. Phys. 61 (1974) 1293.
[28] F.M. Hoffmann, Surf. Sci. Rep. 3 (1983) 107.
[29] P. Sjovall, S.K. So, B. Kasemo, R. Franchy, W. Ho, Chem. Phys. Lett. 171 (1990) 125.
[30] D.A. Outka, R.J. Madix, G. Fisher, C. Dimaggio, Surf. Sci. 179 (1987) 1.
[31] I.C. Hisatsune, J.P. Devlin, Y. Wada, J. Chem. Phys. 33 (1960) 714.
[32] R.V. St. Louis, R. Crawford, J. Chem. Phys. 42 (1965) 857.
[33] A. Givan, A. Loewenschuss, J. Chem. Phys. 93 (1990) 7592.
[34] J.D.S. Goulden, D.J. Millen, J. Chem. Soc. (1950) 2620.
[35] D.W.A. Sharp, J. Thorley, J. Chem. Soc. (1963) 3557.
[36] V.R. Morris, S. Bhatia, J.H. Hall, J. Phys. Chem. 94 (1990) 7414.
[37] R. Vogt, B.J. Finlayson-Pitts, J. Phys. Chem. 98 (1994) 3747.
[38] R. Varma, R.F. Curl, J. Phys. Chem. 80 (1976) 402.
[39] S. Mertes, A. Wahner, J. Phys. Chem. 99 (1995) 14000.
[40] G.E. McGraw, D.L. Bernitt, I.C. Hisatsune, J. Chem. Phys. 45 (1966) 1392.
[41] H. Cohn, C.K. Ingold, H.G. Poole, J. Chem. Soc. (1952) 4272.
[42] M.A. Tolbert, A.M. Middlebrook, J. Geophys. Res. 95 (1990) 22423.

[43] J.S. Robertshaw, I.W.M. Smith, J. Phys. Chem. 86 (1982) 785.
[44] B.M. Cheng, J.W. Lee, Y.P. Lee, J. Phys. Chem. 95 (1991) 2814.
[45] L. Parts, J.T. Miller, J. Chem. Phys. 43 (1965) 136.
[46] A. Given, A. Loewenschuss, J. Chem. Phys. 91 (1989) 5126.
[47] F. Bolduan, H.J. Jodl, Chem. Phys. Lett. 85 (1982) 283.
[48] D.A. Pinnick, S.F. Agnew, B.I. Swanson, J. Phys. Chem. 96 (1992) 7092.
[49] S.F. Agnew, B.I. Swanson, L.H. Jones, D. Schiferl, J. Phys. Chem. 87 (1983) 5065.
[50] A. Given, A. Loewenschuss, J. Chem. Phys. 93 (1990) 866.
[51] A. Given, A. Loewenschuss, J. Chem. Phys. 90 (1989) 6135.
[52] F. Bolduan, H.J. Jodl, A. Loewenschuss, J. Chem. Phys. 80 (1984) 1739.
[53] A. Given, A. Loewenschuss, J. Chem. Phys. 94 (1991) 7562.
[54] T.G. Koch, A.B. Horn, M.A. Chesters, M.R.S. McCoustra, J.R. Sodeau, J. Phys. Chem. 99 (1995) 8362.
[55] P.A. Thiel, T.E. Madey, Surf. Sci. Rep. 7 (1987) 211.
[56] D.R. Hanson, J. Phys. Chem. 99 (1995) 13059.
[57] D.C. Clary, Science 271 (1996) 1509.